

A convolutional neural network for seismic dip estimation

Dawei Liu*, Xiaokai Wang, Zhensheng Shi, Yanhui Zhou, Wenchao Chen, Xi'an Jiaotong University, National Engineering Laboratory for Offshore Oil Exploration, Xi'an, China

Summary

The seismic volumetric dip is widely used in the horizon and fault interpretation. One of the mostly used dip estimating method is the waveform similarity-scanning-based dip estimation which can deliver the reliable dip estimation. However, the waveform similarity-scanning-based (WSSB) dip estimation is computationally intensive. In this abstract, we tried to use deep learning to increase the seismic dip estimation's efficiency. We considered the seismic volumetric dip estimation problem as one convolutional neural networks (CNN) regression problem, and proposed a multi-layer convolutional neural network for seismic dip estimation CNN (SDE-CNN). The proposed SDE-CNN can estimate x-direction apparent dip and y-direction apparent dip spontaneously. Finally, we applied the proposed SDE-CNN to one 3D field seismic dataset. Part of the original seismic dataset and corresponding WSSB dip estimation results are adopted as the training pairs to train our SDE-CNN. The trained SDE-CNN was applied to the rest of 3D field seismic dataset to estimate apparent dips. The results show our SDE-CNN can obtain a similar result with the WSSB dip estimation but use less time than the WSSB dip estimation. The curvature estimations based on our SDE-CNN result and the WSSB dip estimation result also show the accuracy of our SDE-CNN-based dip estimation.

Introduction

Seismic attributes can be used to help interpreters to explore geologic and reservoir engineering information from the seismic dataset. Taner et al. had divided seismic attributes into two categories: geometric attributes and physical attributes (1994). Geometric attributes are frequently used to identify the strata's geometric characteristics, such as fault orientation and channels. As one of the most import geometric attributes, seismic volumetric dip not only can be used to describe tiny geologic structures, but also can be helpful for other important seismic interpretation, such as seismic curvature, structure-oriented filter, coherence, and similarity computation.

Many methods have been proposed to estimate the seismic volumetric dip in the past few decades. Bahorich and Farmer (1995) obtained the seismic volumetric dip by calculating the maximum value of 3D crosscorrelation coherence estimation. Barnes (2007) estimated the seismic volumetric dip by computing the partial derivative of the instantaneous phase which was obtained from the complex

trace analysis. Marfurt et al. (1998) proposed the WSSB, dip estimation which calculates similarity along with a series of preset dips and chooses the dip which has the largest similarity value as the seismic volumetric dip. Structure tensor (Bakker, 2002) was also applied to estimate the seismic volumetric dip and had been widely used in applications. Wu and Janson (2017) proposed one seismic volumetric dip estimating method by utilizing directional structure tensors. Marfurt (2006) adopted multiple-analysis-window technology to estimate the seismic dip by selecting the neighboring windows which produce the largest coherence. Fomel (2002) estimated seismic dip by establishing plane-wave destruction filters. Besides, Marfurt and Kirlin (2000) introduced multiple signal classification (Schmidt, 1986) from radar signal processing to estimate seismic dip. Among these dip estimating method, the WSSB dip estimation can deliver one reliable dip estimation if the dip scanning interval is small enough. However, the waveform similarity-scanning-based dip estimation is computationally intensive for a small dip scanning interval. Therefore, how to balance the accuracy and consuming time should be considered for the WSSB dip estimation.

In recent years, deep learning has made tremendous progress in image recognition due to its outstanding feature extraction ability. Parkhi et al. (2015) used CNN for face recognition (Parkhi, 2015). Baccouche et al. incorporated CNN and recurrent neural network for human action recognition (Baccouche, 2011). Besides, CNN was also applied to scene recognition (Zhou, 2014) and speech recognition (Abdel-Hamid, 2014). Many researchers have introduced deep learning into seismic signal processing as an effective alternative way to classic seismic processing method. Araya-Polo et al. (2017) proposed a deep learning system to identify fault automatically and gained accurate predictions with the use of Wasserstein loss function. Shi et al. (2018) proposed an algorithm for detecting the salt body in seismic images and found the network could extract essential information from training samples. Pham et al. (2018) applied an encoder-decoder network for channel detection and found the network can identify the channel bodies in the field dataset with the network trained on the synthetic dataset.

Inspired by the theorem that the neural network can approximate any arbitrary continuous function, we try to use one deep neural network to learn the mapping relationship between the original 3D seismic dataset and the WSSB dip estimation's result. In this work, we try to utilize an SDE-CNN to estimate the seismic volumetric dip. Firstly, we will introduce the WSSB dip estimation briefly.

A convolutional neural network for seismic dip estimation

Then we will give the SDE-CNN's architecture and training strategy. Finally we applied our CNN to a 3D field dataset. Part of the 3D field dataset and corresponding WSSB dip estimation's result are used to train the proposed CNN, while the rest of the 3D field dataset is used to test the performance of our trained SDE-CNN. Our trained SDE-CNN not only obtain a comparable result with the WSSB dip estimation's result, but also greatly reduce the computing time from hours to minutes.

Method

If we treat the seismic dip estimation problem as one classification problem, x-direction dip estimation output classification types should more than 1000 in order to obtain a higher resolution. This will result in a large amount of calculation in the last fully connected layer, which will drastically increase the calculation time. Since traditional methods always estimate the seismic dip within one sliding window, we can treat the dip estimation problem as a nonlinear regression task which can use CNN to approximate a nonlinear mapping between the original seismic dataset and the result of WSSB dip estimation. In this section we will briefly introduce the WSSB dip estimation, and then present a 3D SDE-CNN's architecture. Finally, we build some training datasets and feed the network.

The WSSB dip estimation

One 3D migrated volume can be represented by $u(t, x, y)$, where t , x , and y represent the corresponding indexes along t -direction, x -direction, and y -direction, respectively. We can easily obtain the image part $u^H(t, x, y)$ through complex trace analysis. Suppose the size of time window has $2M+1$ samples and there are J traces in one analyzing window, we can compute the focusing point (t, x, y) 's waveform similarity with the following formula Marfurt et al. (1998, 2000):

$$S(\theta_x, \theta_y) = \frac{\sum_{n=-M}^M \left\{ \left[\sum_{j=1}^J u(t-n-\theta_x x - \theta_y y) \right]^2 + \left[\sum_{j=1}^J u^H(t-n-\theta_x x - \theta_y y) \right]^2 \right\}}{\sum_{n=-M}^M \left\{ \sum_{j=1}^J [u(t-n-\theta_x x - \theta_y y)]^2 + \sum_{j=1}^J [u^H(t-n-\theta_x x - \theta_y y)]^2 \right\}}. \quad (1)$$

Here θ_x and θ_y are the preset apparent dips along x-direction and y-direction, respectively. If we change θ_x and θ_y from $-\theta_{max}$ to θ_{max} with a small dip interval, we can obtain a series of similarities. Then the dip pair with the maximum similarity is chosen as the focusing point (t, x, y) 's apparent dip. Besides, the apparent dip can be improved by fitting a 2D paraboloid through the nine discretely sampled points neighboring the point having the maximum similarity (Marfurt, 2000).

Network architecture

The input of our SDE-CNN is the original 3D seismic data volume \mathbf{u} . The outputs of our SDE-CNN are the estimated dips \mathbf{d} which include the apparent dips along x-direction and y-direction. We employ the CNN to train a direct mapping $R(\mathbf{u}) \approx \mathbf{d}$ which maps the input seismic data to seismic dip. The averaged mean squared error between the desired seismic dip \mathbf{d}' and the estimated dip $R(\mathbf{u})$ from input seismic data is set as loss function L . The purpose of L is to make the estimated dip \mathbf{d} and label \mathbf{d}' as similar as possible. The corresponding formula of L can be written as:

$$L(\Theta) = \frac{1}{2N} \sum_{i=1}^N \|R(\mathbf{u}_i; \Theta) - \mathbf{d}'_i\|_F^2. \quad (2)$$

Here $\{(\mathbf{u}_i, \mathbf{d}')\}$ represents the i -th training pair and N represents the total number of training sample pairs. The network input \mathbf{u} and label \mathbf{d}' are different type datasets, some regularization constraints can be added to make the training procedure coverage easily. We use the back-propagation method (Rumelhart et al., 1986) to find a locally-optimal of the trainable parameters after iterative training.

Fig.1 shows the specific architecture of our 3D SDE-CNN. The SDE-CNN regression model has one four-stage structure. The first stage and last stage is composed of one convolutional layer. Inspired by the empirical parameter setting in VGG-net (Simonyan and Zisserman, 2014), we choose the size of convolutional kernel to be $3 \times 3 \times 3$ and delete all pooling layers to make the output size meet our requirement. The second stage is composed of seven convolutional layers, and each of them is followed by a batch normalization layer. The batch normalization is adopted for accelerating training convergence and improving estimating performance in our method. The third stage is composed of ten convolutional layers. We use valid padding at intervals to make full use of input information while reducing the size of network output. In the process of convolution calculation, in order to allow the data on the boundary to participate in the convolution calculation as a center, it is necessary to pad the boundary. There are many kinds of padding operations such as zero padding, symmetric boundary padding, and periodic padding. If valid padding is adopted, the output size of the convolution layer will be smaller than the input size. Reducing network output can ensure each voxel of output dataset has enough receptive field to obtain valid information of seismic data.

Model training strategy

There are 681 lines, 401traces in our 3D field dataset. We use the WSSB dip estimation to estimate the seismic apparent dips along x-direction and y-direction. The dip searching range is from -4 to 4 and the dip searching interval is 0.125. The first 150 lines of the original dataset are selected for training, while the first 150 lines of the

A convolutional neural network for seismic dip estimation

estimated apparent dip estimation are selected as the corresponding ground-truth labels. Then we cut the training dataset and corresponding labels into small cubes to construct training samples set. When we feed these seismic cubes and their corresponding labels into our SDE-CNN, the network will learn the right way to estimate seismic apparent dip from the original raw seismic dataset.

The first two stages of SDE-CNN are used for extracting high-level abstractions of input seismic data. These abstractions for x-direction are same as these abstractions for y-direction. Therefore, to reduce the computation cost, we duplicate the third stage of SDE-CNN so that the network can simultaneously output the apparent dip along x-direction and y-direction. The procedure of our CNN-based dip estimation is shown in Fig. 2.

Examples

We use the trained SDE-CNN to estimate the apparent dip of the rest 531 lines. First we will show the efficiency of WSSB dip estimation and our SDE-CNN. When we adopt the WSSB dip estimation to estimate the seismic dip, we set the dip searching range as $[-4, 4]$ and the dip searching interval as 0.125. The C++ program run on a workstation with the following specifications: an Intel(R) Xeon(R) E5-1620 v3 @3.50 GHz and 32 GB RAM. This parallel program employs four cores, and the total consuming time of WSSB dip estimation is 4.7 hours. When we use the trained SDE-CNN to the same 3D dataset, the total consuming time is about 6 minutes. Therefore, our SDE-CNN is more efficient than the commonly-used WSSB dip estimation.

Fig. 3 shows the slice comparison. Fig.3a and Fig.3b show two time slices of the x-direction dip estimation results based on WSSB dip estimation and our trained SDE-CNN. Besides the area near data boundary, there is no visible difference between the result of WSSB dip estimation and the dip estimation result based on our trained SDE-CNN.

Furthermore, Fig.3b (the result of our trained SDE-CNN) has a sharper channel edge which is indicated by the orange ellipse. In order to further evaluate our trained SDE-CNN's result, we also calculate the difference between the WSSB dip estimation's result and our SDE-CNN result. The time slice of the difference cube is shown in Fig.3c. Although there is some visible difference near some big faults, the errors of other position are very small. We guess the visible difference near big faults may be caused by the limited dip searching range. To test the performance of our SDE-CNN in detail, we use structural curvature, which is calculated based on the partial derivatives of apparent dips. The corresponding slices of the most negative curvature based on WSSB dip estimation and our SDE-CNN result are shown in Fig. 4. We can also observe our SDE-CNN can generate a comparable curvature result with the curvature result based on WSSB dip estimation except for the area near the boundary.

Conclusions

In this abstract, we proposed a seismic dip estimation method based on deep learning. We introduce a convolutional regression model to map the post-stack seismic dataset to the estimated dip. The network is trained and tested on the field seismic dataset. Compared with the traditional dip estimation method, our well-trained CNN can greatly save the computing time and generate a comparable dip estimation result except for boundary area.

Acknowledgments

The research was funded by National Natural Science Foundation of China (41774135, 41504092, and 41504093), China Postdoctoral Science Foundation (2016T90925), National Key Research and Development Program of China (2017YFB0202902), and the Fundamental Research Funds for the Central Universities. We would like to thank Daqing oilfield for providing the dataset.

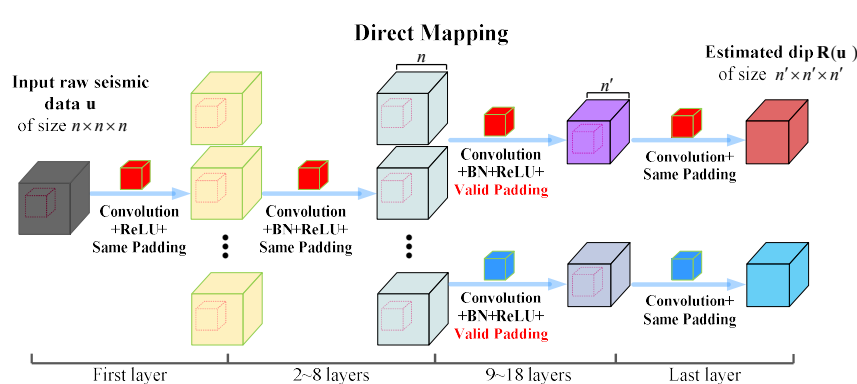


Fig. 1. The network structure of our seismic dip estimation CNN.

A convolutional neural network for seismic dip estimation

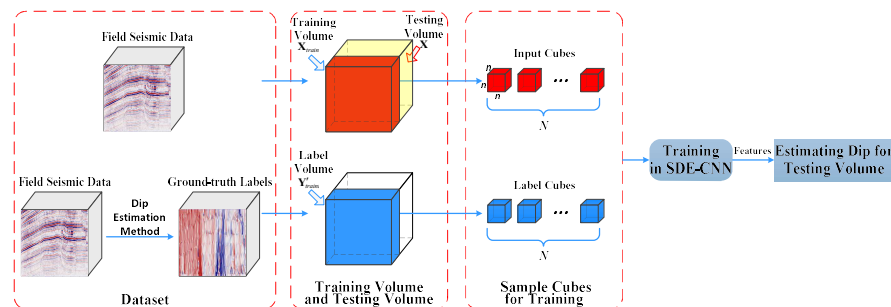


Fig. 2. The procedure of our CNN-based dip estimation.

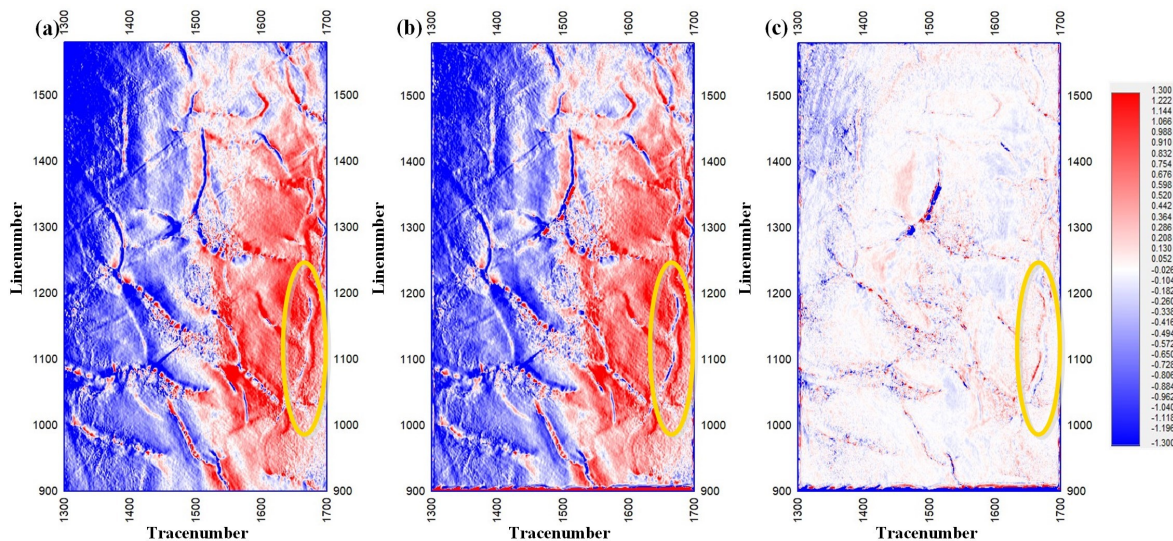


Fig. 3. The time slices of (a) the WSSB dip estimation result, (b) our trained CNN result, and (c) the difference between (a) and (b).

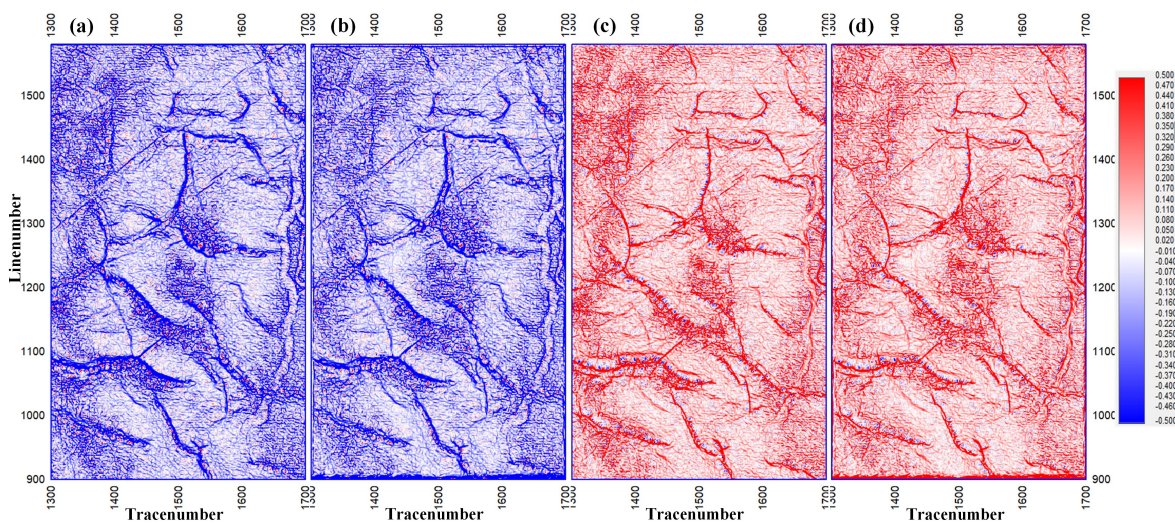


Fig. 4. Time slices of the most negative curvature based on (a) the WSSB dip estimation and (b) our trained CNN result, and two time slices of the most positive curvature based on (c) the WSSB dip estimation and (d) our trained CNN result.

REFERENCES

- Abdel-Hamid, O., A.-R. Mohamed, H. Jiang, L. Deng, G. Penn, and D. Yu, 2014, Convolutional neural networks for speech recognition: IEEE/ACM Transactions on Audio, Speech, and Language Processing, **22**, 1533–1545, doi: [10.1109/TASLP.2014.2339736](https://doi.org/10.1109/TASLP.2014.2339736).
- Araya-Polo, M., T. Dahlke, C. Frogner, C. Zhang, T. Poggio, and D. Hohl, 2017, Automated fault detection without seismic processing: The Leading Edge, **36**, 208–214, doi: [10.1190/tle36030208.1](https://doi.org/10.1190/tle36030208.1).
- Baccouche, M., F. Mamalet, C. Wolf, C. Garcia, and A. Baskurt, 2011, Sequential deep learning for human action recognition: International Workshop on Human Behavior Understanding, 29–39.
- Bahorich, M. S., and S. L. Farmer, 1995, 3-D seismic discontinuity for faults and stratigraphic features: The coherence cube: 65th Annual International Meeting, SEG, Expanded Abstracts, 93–96, doi: [10.1190/1.1437077](https://doi.org/10.1190/1.1437077).
- Bakker, P., 2002, Image structure analysis for seismic interpretation: Delft University of Technology.
- Barnes, A. E., 2007, A tutorial on complex seismic trace analysis: Geophysics, **72**, no. 6, W33–W43, doi: [10.1190/1.2785048](https://doi.org/10.1190/1.2785048).
- Fomel, S., 2002, Applications of plane-wave destruction filters: Geophysics, **67**, 1946–1960, doi: [10.1190/1.1527095](https://doi.org/10.1190/1.1527095).
- Marfurt, K. J., 2006, Robust estimates of 3D reflector dip and azimuth: Geophysics, **71**, no. 4, P29–P40, doi: [10.1190/1.2213049](https://doi.org/10.1190/1.2213049).
- Marfurt, K. J., and R. L. Kirlin, 2000, 3-D broad-band estimates of reflector dip and amplitude: Geophysics, **65**, 304–320, doi: [10.1190/1.1444721](https://doi.org/10.1190/1.1444721).
- Marfurt, K. J., R. L. Kirlin, S. L. Farmer, and M. S. Bahorich, 1998, 3-D seismic attributes using a semblance-based coherency algorithm: Geophysics, **63**, 1150–1165, doi: [10.1190/1.1444415](https://doi.org/10.1190/1.1444415).
- Parkhi, O. M., A. Vedaldi, and A. Zisserman, 2015, Deep face recognition: British Machine Vision Conference, 1, 6.
- Pham, N., S. Fomel, and D. Dunlap, 2018, Automatic channel detection using deep learning: 88th Annual International Meeting, SEG, Expanded Abstracts, 2026–2030, doi: [10.1190/segam2018-2991756.1](https://doi.org/10.1190/segam2018-2991756.1).
- Rumelhart, D. E., G. E. Hinton, and R. J. Williams, 1986, Learning representations by back-propagating errors: Nature, **323**, 533.
- Schmidt, R., 1986, Multiple emitter location and signal parameter estimation: IEEE Transactions on Antennas and Propagation, **34**, 276–280, doi: [10.1109/TAP.1986.1143830](https://doi.org/10.1109/TAP.1986.1143830).
- Shi, Y., X. Wu, and S. Fomel, 2018, Automatic salt-body classification using a deep convolutional neural network: 88th Annual International Meeting, SEG, Expanded Abstracts, 1971–1975, doi: [10.1190/segam2018-2997304.1](https://doi.org/10.1190/segam2018-2997304.1).
- Simonyan, K., and A. Zisserman, 2014, Very deep convolutional networks for large-scale image recognition: arXiv preprint arXiv:1409.1556.
- Taner, M. T., 1994, Seismic attributes revisited: 64th Annual International Meeting, SEG, Expanded Abstracts, 1104, doi: [10.1190/1.1822709](https://doi.org/10.1190/1.1822709).
- Wu, X., and X. Janson, 2017, Directional structure tensors in estimating seismic structural and stratigraphic orientations: Geophysical Journal International, **210**, 534–548, doi: [10.1093/gji/ggx194](https://doi.org/10.1093/gji/ggx194).
- Zhou, B., A. Lapedriza, J. Xiao, A. Torralba, and A. Oliva, 2014, Learning deep features for scene recognition using places database: Advances in Neural Information Processing Systems.